



Universiteit
Leiden
The Netherlands

Advances in SQUID-detected magnetic resonance force microscopy

Wit, M. de

Citation

Wit, M. de. (2019, June 18). *Advances in SQUID-detected magnetic resonance force microscopy*. *Casimir PhD Series*. Retrieved from <https://hdl.handle.net/1887/74054>

Version: Not Applicable (or Unknown)

License: [Leiden University Non-exclusive license](#)

Downloaded from: <https://hdl.handle.net/1887/74054>

Note: To cite this publication please use the final published version (if applicable).

Cover Page



Universiteit Leiden



The handle <http://hdl.handle.net/1887/74054> holds various files of this Leiden University dissertation.

Author: Wit, M. de

Title: Advances in SQUID-detected magnetic resonance force microscopy

Issue Date: 2019-06-18

1

INTRODUCTION

In this thesis, we will cover some of the latest advances in Magnetic Resonance Force Microscopy, a technique that detects the tiny forces exerted by electrons or nuclei to obtain information about the structure or properties of a wide variety of samples. In this chapter, we give a coarse overview of the history of MRFM, followed by the motivation of the strategy followed by the Oosterkamp group to improve upon the existing technique. We end by giving an outline for the rest of this work.

1.1 DEVELOPMENT AND APPLICATIONS OF MRFM

The concept of Magnetic Resonance Force Microscopy was first described by Sidles, who envisioned MRFM as a technique that might resolve the structure of biological samples, such as proteins or virus particles [1]. Traditionally, these kinds of samples were studied using X-ray crystallography or Nuclear Magnetic Resonance (NMR) [2]. However, these techniques suffer from a number of drawbacks that limit the number of structures that can be resolved. As an example, NMR and the related Magnetic Resonance Imaging (MRI) use a radio-frequency magnetic field to excite the nuclear spins in a sample and measure their properties. The weak interactions between these fields and spins allow the samples to be investigated in a non-invasive way. However, the weak interaction also means that these techniques are inherently insensitive, and therefore require a large number of spins to generate a sufficiently large signal to be detected. Sidles suggested that the sensitivity of NMR could be enhanced by uniting it with Atomic Force Microscopy (AFM). This combined technique would use spin manipulation protocols from NMR, but the resulting state of the spins in the proteins would be detected by measuring forces using a mechanical resonator.

From this original conception in 1991, progress was quick. In 1992, the first Electron Spin Resonance (ESR) signal was detected by Rugar et al. [3], soon to be followed by the first successful imaging of a sample of the organic chemical compound DPPH with a lateral resolution of 5 μm [4]. Even though the signal from nuclear spins is almost three orders of magnitude smaller than that from electrons, the first nuclear MRFM experiment on protons was achieved in 1994, once again by Dan Rugar and colleagues at IBM [5]. Via the development of ever more sensitive cantilevers for the detection of the force signals [6, 7] and more sophisticated protocols to manipulate the spins [8–11], in 2004 single electron spin sensitivity was demonstrated [12]. With the goal of single electron spin resolution achieved, more effort was invested in optimizing the sensitivity for nuclear experiments [13, 14], including isotope-selective imaging [15]. The experiment that came closest to Sidles' original idea was performed in 2009, when Degen et al. managed to create a three-dimensional reconstruction of the Tobacco Mosaic Virus (TMV) with a spatial resolution better than 5 nm [16]. At the moment, the record for the spatial resolution (in one dimension) is set at 2 nm using a polystyrene-coated silicon nanowire [17]. Between 1992 and 2018, the sensitivity of MRFM has been improved by seven orders of magnitude, equivalent to a doubling of the sensitivity on average every 21 months during this period.

Note that during this development of imaging using MRFM, many groups often switched from the sample-on-tip geometry, in which the sample is attached to the cantilever and is then positioned near a small nanomagnet (pioneered by the IBM

group), to the magnet-on-tip geometry, in which the nanomagnet is attached to the cantilever and positioned near a sample (first used by Wago et al. [18] and Bruland et al. [19]), and back. In principle the sample-on-tip geometry has the best prospects for the application of imaging, as this approach is less sensitive to effects that reduce the quality factor of the cantilever, and higher magnetic field gradients can be achieved using surface-mounted nanomagnets. For this reason, this was the geometry used for the TMV experiment. However, this geometry severely limits the generality of the samples that can be investigated. The desire for generality favors the magnet-on-tip geometry, since having the sample on a surface other than the cantilever allows for more flexibility in terms of sample preparation.

Recent progress towards imaging has been slow compared to the early years. When we take the work by Mamin et al. on CaF_2 from 2007 as an intermediate benchmark, we find that in the period 1992-2007 the sensitivity doubled on average every 15 months, while in the period 2007-2018 this only happened every 51 months. It took 9 years for a group to improve upon the 5 nm resolution achieved in the TMV experiment. As is often the case with new technologies, the initial steps to increase the performance are clear and significant. However, keeping up the high rate of progress is extremely challenging, and it is unclear how to move from the ideal proof-of-principle systems to the real-world samples. Furthermore, imaging based on MRFM seems to have lost momentum compared to other techniques, such as (three-dimensional) electron microscopy techniques [20–24] and (scanning) NV-centers [25–27].

Now, this is not to say that MRFM has run its course. An alternative application of MRFM has gained popularity, namely to investigate condensed matter samples. Research is done on a variety of phenomena, such as ferromagnetic resonance [28–31], spin diffusion in strong field gradients [32–34], and spin-lattice relaxation times in small samples [35–37]. In our group, we try to take advantage of our low operating temperatures in combination with the capability to measure sub-surface effects. For these reasons, Wagenaar has suggested experiments on LAO-STO, high-temperature superconductors, and 3D topological insulators [37, 38].

1 1.2 PRINCIPLES OF MRFM

To understand the main principle of MRFM, we can simply deconstruct the name of the technique:

MAGNETIC: Consider a single spin with magnetic moment $\mu_s = S\hbar\gamma$, where S is the spin quantum number, \hbar is the reduced Planck constant, and γ is the gyromagnetic ratio, an isotope-dependent constant. For simplicity we will consider spins with $S = 1/2$, as is the case for electrons and protons. When we place the spin in a static magnetic field B_0 , the spin aligns either parallel (“up”) or anti-parallel (“down”) to this field, where the anti-parallel state has a slightly higher energy than the parallel state, with the energy difference given by $\Delta E = 2\mu_s B_0$.

RESONANCE: The spin can be manipulated using an alternating magnetic field B_1 (also called B_{RF}), but only when the frequency of this field matches the Larmor frequency of the spin, given by $\omega_L = \gamma|B_0|$. Equivalently, one can say that the energy of the pulse has to match the energy difference between the spin states. When the spin is positioned in the proximity of a small magnetic particle, the B_0 field varies spatially, which means the Larmor frequency of the spin becomes a function of position with respect to the magnetic particle. In that case, the frequency of the B_1 field, ω_{RF} , can be used to determine the distance of the spin to the magnetic particle.

FORCE: The magnetic moment of the spin is detected via the force it exerts when placed in a magnetic field gradient, such as the one created by the a small magnetic particle. The force is then given by $F = \mu_s (\nabla \cdot \mathbf{B}_0) \equiv \mu_s G$. In a field gradient $G = 0.1$ MT/m, the force exerted by a single spin ranges from 10^{-21} N for nuclear spins to 10^{-17} N for electron spins. These minute forces are detected by placing either the sample or the magnet at the end of a very soft cantilever. The force exerted by the sample on the tip results in a displacement of the cantilever tip, which can be detected using, for instance, a laser reflecting from the surface of the cantilever.

MICROSCOPY: The principles outlined above for the detection of a single spin remain valid when we consider an ensemble of spins. Again, the spins will align in the B_0 field either in the up or down state, where the population difference between the states is dictated by the Boltzmann polarization. For $S = 1/2$ particles, the equilibrium distribution follows from statistical mechanics, and is described by $N_+/N_- = e^{-(\mu_s B_0/k_B T)}$,

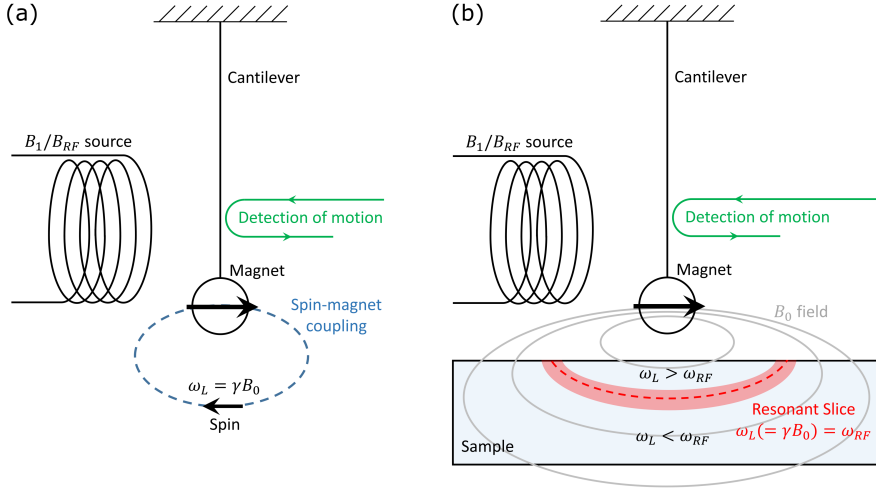


Figure 1.1: (a) Schematic of the MRFM setup and a single spin. The vital components of the setup are shown: the cantilever, B_1 field source, a detection mechanism (e.g. laser interferometer), and a small magnetic particle. (b) Schematic of the MRFM setup indicating the resonant slice, the region in space where $\omega_{RF} = \gamma B_0$.

where N_+/N_- is the ratio of spin up to spin down, $k_B = 1.38 \cdot 10^{-23}$ J/K is the Boltzmann constant, and T is the temperature of the spin ensemble. The signal now originates from all spins within the volume of space where $\gamma B_0 = \omega_{RF}$, the so-called resonant slice. This means that the spatial location of the addressed spins can be controlled by changing the frequency of the B_1 field, or by changing the position of the sample with respect to the magnet. It is possible to make a three-dimensional image of the sample by measuring the force signal for various positions of the magnet with respect to the sample. The resulting force map can be translated to a spin-density map using a deconvolution procedure [16, 39, 40]. The high field gradients mean that this reconstruction can have a spatial resolution as small as several nanometers.

The described measurement principle is shown in Fig. 1.1. The figure shows the so called “magnet-on-cantilever” geometry that is used in the rest of this thesis. Fig. 1.1(a) shows the vital components of an MRFM setup: a soft cantilever as force sensor, a source for the B_1 field required to manipulate the spin, a detection mechanism to read out the motion and properties of the cantilever, and a small magnet to generate large magnetic field gradients which are the origin of the force interaction, and give MRFM its high spatial resolution. In our case, the small magnet is also responsible for the generation of the B_0 field, as we do not apply an additional external magnetic field. Fig. 1.1(b) shows an example of a resonant slice. Only spins within this slice are resonant with the applied B_1 field and contribute to the signal.

1.3 SENSITIVITY LIMIT AND THE OOSTERKAMP APPROACH

As MRFM is inherently a force-detection technique, the fundamental limit for the sensitivity is set by the thermal force noise. The thermal force noise for a cantilever is given by:

$$\sqrt{S_F} = \sqrt{4k_B T \Gamma BW} = \sqrt{4k_B T \frac{k_0}{\omega_0 Q} BW}, \quad (1.1)$$

where Γ is the damping rate, k_0 is the stiffness of the cantilever, $\omega_0 = 2\pi f_0$ is its resonance frequency, Q is the quality factor, and BW is the measurement bandwidth. This force noise induces thermal fluctuations of the cantilever position as well as frequency noise. Using the force exerted by a magnetic moment in a magnetic field gradient we find that the minimal detectable magnetic moment in a unit bandwidth is given by:

$$\mu_{\min} = \frac{1}{G} \sqrt{4k_B T \frac{k_0}{\omega_0 Q}} \quad (1.2)$$

From this equation, it is clear that there are several routes to take if one wants to increase the sensitivity of MRFM. First, one should maximize the magnetic field gradients, which range from about 0.1 - 30 MT/m [19, 41, 42]. We take a closer look at how to maximize the magnetic field gradient in Ch. 8. Second, one has to use a cantilever with extreme dimensions (very long, very thin, and narrow) to minimize k/ω_0 , and with a very low intrinsic damping to obtain a high quality factor. This last requirement is often at odds with the demand that cantilevers are thin [43]. Finally, the temperature of the resonator has to be as low as possible, as this means a lower average thermal energy.

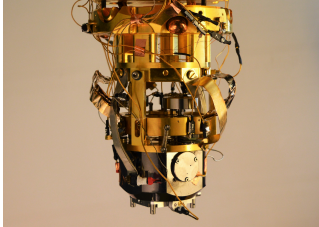
THE OOSTERKAMP APPROACH: Our main focus is to reduce the operating temperature of the MRFM setup. The low temperature not only reduces the force noise, but is also useful for reducing the relaxation rates of spins and increasing the Boltzmann polarization, and thereby the signal when Boltzmann-based protocols are used (as discussed in Ch. 4). There are multiple MRFM setups in the world that are operated in a dilution refrigerator, but this is not enough to achieve true milliKelvin temperatures in full operation. Several technical innovations to the setup are required to achieve this:

- The temperature of the cantilever in conventional MRFM is limited by the power input from the laser used for the read-out of the cantilever motion. Even for incident laser powers as low as 1 nW, no effective cantilever temperatures below 100 mK have been reported using laser read-out [44–46]. For this reason, we have implemented a SQUID-based detection scheme. Here the motion of the cantilever is measured using a superconducting pickup loop connected to a SQUID that detects the flux changes from the moving magnet at the end of the cantilever. Using this scheme, cantilever temperatures below 20 mK have been achieved [47, 48]. Details about this scheme are given in Ch. 2.
- Apart from thermal fluctuations, the cantilever can also be excited by mechanical vibrations, for instance originating from the cryostat. A sophisticated vibration isolation is required to provide sufficient attenuation of external vibration at the cantilevers resonance frequency. However, often the (soft) vibration isolation reduces the thermal conductance between the MRFM setup and the cooling mechanism, e.g., the mixing chamber of a dilution refrigerator. Therefore, we have developed a mechanical vibration isolation that combines good vibrational properties with a high thermal conductance, as discussed in Ch. 3.
- It has proven very challenging to generate B_1 fields of sufficient amplitude for many MRFM protocols without significant dissipation. We have attempted to reduce this dissipation by using a superconducting microwire as source for the B_1 field [37, 49]. Furthermore, we have developed a method for the mechanical generation of RF fields using the higher modes of the cantilever [50]. This approach will be further discussed in Ch. 4.

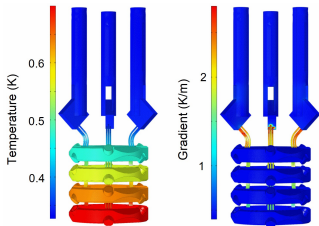
Using these technical innovations, the Oosterkamp group currently has the only operational setup in which a temperature down to 20 mK for both the cantilever and the sample is achieved during MRFM experiments. However, it has been found that the low temperatures also pose significant challenges. Spin-mediated dissipation of the cantilever energy, resulting in lower quality factors, is an increasingly important effect at lower temperatures [34, 51, 52]. Furthermore, even though we use a superconducting RF source, significant dissipation is observed even for modest RF amplitudes and frequencies, as discussed in Ch. 7.

1.4 THESIS OUTLINE

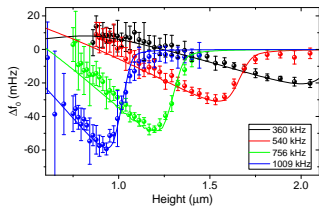
The thesis is structured as follows.



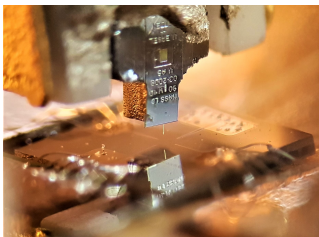
CHAPTER 2 introduces the experimental setup. It covers the most important components, such as the detection chip and the magnetically-tipped cantilever. The cantilever's response to a driving force is described starting from the equations of motion. Subsequently, it covers the positioning stages and methods, and the modifications made to the dilution refrigerator.



CHAPTER 3 presents the newly developed vibration isolation. It starts from a general design principle based on the analogy between electrical and mechanical filters, followed by a detailed account of the final implementation. The effectiveness is shown using SQUID vibration spectra and the cantilever's thermal properties.

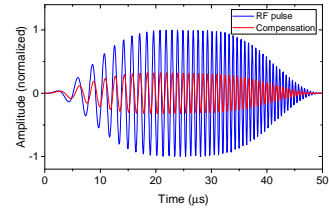


CHAPTER 4 shows the feasibility of Boltzmann-polarization-based imaging in MRFM. We study the time-dependent behaviour of both on- and off-resonant spins when excited by RF magnetic fields. The results are confirmed using frequency shift signals measured using the mechanical generation of RF fields. A volume sensitivity of $(40 \text{ nm})^3$ is achieved. We end with estimates of the expected volume resolution for a proton sample.

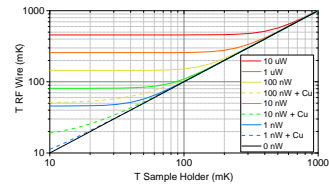


CHAPTER 5 is devoted to the study of surface and bulk spins in diamond. Ultra sensitive magnetic force microscopy at milliKelvin temperatures reveals that a high magnetic field gradient suppresses spin diffusion, increasing relaxation times of surface spins. The technique offers a valuable tool for characterizing dilute spin systems, which could yield insight on how to reduce dissipation in qubits and other nanodevices.

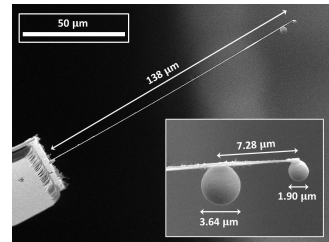
CHAPTER 6 describes the developed flux compensation scheme used to reduce the crosstalk between the SQUID-based read-out and the generated RF fields. The full electrical scheme of the RF- and detection circuits is described, together with the operation principle and calibration methods for the compensation. The effectiveness of the cancellation of flux crosstalk is shown by comparing the performance of the SQUID (i.e. modulation depth and noise) with and without an active compensation scheme.



CHAPTER 7 contains calorimeter measurements of the dissipated power when an RF current is passed through a superconducting RF wire. Various sources of dissipation are discussed, such as eddy currents induced in surrounding metals and flux-vortex flow in the superconductor itself. The chapter concludes with a number of suggestions to reduce the dissipated power and to limit the resulting increase in the temperature of the detection chip and sample.



CHAPTER 8 reports on our attempts to obtain higher magnetic field gradients whilst reducing the typically associated drawbacks. It is based on cantilevers with two affixed magnets, one with a small diameter to increase the maximum field gradient and thereby the spin signal, and one with a larger diameter several micrometers away from the tip of the cantilever to maintain a high coupling to the detection mechanism. The chapter presents the basic scaling laws concerning the magnet radius, and calculations of the expected influence on the MRFM experiment.



CHAPTER 9 concludes the thesis with a description of the progress of the easy-MRFM. The proof-of-principle is given, together with suggestions to improve the performance. This new device could make the technique of MRFM more widely available for other research groups, and could shed light on some of the big issues currently plaguing many nanodevices.



